OncoTargets and Therapy

Dovepress
Taylor & Francis Group

Open Access Full Text Article

ORIGINAL RESEARCH

The EphA3 Antibody Enhances CD47 Antibody-Mediated Phagocytosis by Repolarizing M2-Like Tumor-Associated Macrophages in a Preclinical Model of Recurrent Head and Neck Cancer

Song Hee Kim[1,*], Ji Won Kim[1,*], Min Seok Kim[1], Hee Jeong Cha[2], Seong Who Kim[3], Myung Woul Han[1]

[1]Department of Otorhinolaryngology-Head and Neck Surgery, Ulsan University Hospital, University of Ulsan College of Medicine, Ulsan, Korea; [2]Department of Pathology, Ulsan University Hospital, University of Ulsan College of Medicine, Ulsan, Republic of Korea; [3]Department of Biochemistry and Molecular Biology, Asan Medical Center, University of Ulsan College of Medicine, Seoul, Republic of Korea

*These authors contributed equally to this work

Correspondence: Myung Woul Han, Department of Otorhinolaryngology-Head and Neck Surgery, Ulsan University Hospital, University of Ulsan College of Medicine, 877 Bangeojinsunhwan-doro, Dong-gu, Ulsan, 44033, Republic of Korea, Email brightmoon@uuh.ulsan.kr; Seong Who Kim, Department of Biochemistry and Molecular Biology, Asan Medical Center, University of Ulsan College of Medicine, 88 Olympic-Ro 43-Gil, Songpa-Gu, Seoul, 05505, Republic of Korea, Email swhokim@amc.seoul.kr

Background: Head and neck squamous cell carcinoma (HNSCC) is characterized by a highly immunosuppressive tumor microenvironment (TME), with tumor-associated macrophages (TAMs) playing a central role in resistance to therapy. The immune checkpoint molecule CD47, known for its "don't eat me" signal, and EphA3, a receptor tyrosine kinase, are both upregulated in radiation-resistant HNSCC. However, their cooperative role in regulating TAMs and therapeutic resistance remains poorly understood.

Methods: We established a radiation-resistant HNSCC model (MOC2R) using repeated irradiation and confirmed increased expression of CD47 and EphA3 in these cells. The effects of single and dual blockade of CD47 and EphA3 were evaluated through in vitro phagocytosis assays, Western blot, co-immunoprecipitation, and in vivo tumor models. Transcriptomic analysis and immunofluorescence staining were performed to elucidate molecular pathways involved in TAM modulation. We demonstrated in three independent experiments (n = 3) with statistical significance ($P < 0.05$).

Results: CD47 and EphA3 were upregulated in radioresistant HNSCC and recurrent tumors. Dual blockade synergistically enhanced macrophage-mediated phagocytosis ($P < 0.01$) and significantly reduced clonogenic tumor cell survival compared to single blockade ($P < 0.0001$). EphA3 inhibition reprogrammed tumor-associated macrophages toward an M1-like phenotype, with increased expression of pro-inflammatory markers and decreased M2-associated markers. In vivo, combination therapy significantly reduced tumor volume and weight and increased M1 macrophage infiltration, while reducing M2 macrophages. Mechanistically, EphA3 regulated macrophage polarization via the β-catenin/FOSL2/ARID5A axis, enhancing the efficacy of CD47 blockade.

Conclusion: Our findings demonstrate that EphA3, in cooperation with CD47, promotes an immunosuppressive TME by modulating β-catenin/FOSL2/ARID5A signaling in TAMs. Dual targeting of EphA3 and CD47 represents a promising strategy to reprogram macrophages and enhance anti-tumor immunity in radiation-resistant HNSCC.

Keywords: head and neck cancer, recurrence, EphA3, CD47, tumor-associated macrophage, phagocytosis, macrophage

Introduction

Tumor-associated macrophages (TAMs) are critical components of the tumor microenvironment (TME), where they promote immune suppression, angiogenesis, metastasis, and tumor progression by remodeling the TME into an

https://doi.org/10.2147/OTT.S595937
Received: 13 January 2026
Accepted: 27 April 2026
Published: 15 May 2026

immunosuppressive niche.[1–3] Through metabolic reprogramming and support of neoangiogenesis, TAMs interact with both immune and tumor cells to facilitate cancer progression.[2] Their remarkable plasticity enables them to adopt either tumor-promoting (pro-tumorigenic) or tumor-inhibiting (anti-tumorigenic) phenotypes in response to microenvironmental cues. In their pro-tumorigenic state, TAMs promote blood vessel formation, suppress antitumor immunity, and enhance metastatic potential.[4] TAMs are broadly classified into two functional phenotypes: M1 and M2. M1 macrophages, or classically activated macrophages, are associated with pro-inflammatory responses and tumoricidal activity, while M2 macrophages, alternatively activated, contribute to tumor growth, immune suppression, tissue remodeling, and angiogenesis.[5] Several signaling pathways regulate this polarization process, including the STAT family,[6] PI3K-r/AKT,[7] NF-kB,[8] and the CD47/SIRPa axis.[9] Understanding the mechanisms that drive TAM polarization is crucial for developing therapeutic strategies aimed at reprogramming M2-like TAMs toward a tumor-inhibitory M1 phenotype.

Therapeutic strategies targeting TAMs include inhibiting their recruitment, depleting them, or reprogramming their function.[10] Blocking recruitment prevents TAM infiltration into tumors; depletion removes existing macrophages through apoptosis or immune-mediated clearance. Reprogramming, however, leverages macrophage plasticity to convert immunosuppressive M2 macrophages into pro-inflammatory, antitumor M1 macrophages,[2,10] thereby enhancing the host's immune response.

CD47, a cell-surface protein widely expressed on tumor cells, functions as a "don't eat me" signal by engaging signal regulatory protein alpha (SIRPα) on macrophages and inhibiting phagocytosis. Therapeutic blockade of CD47–SIRPα signaling restores the ability of macrophages to recognize and eliminate tumor cells, and has shown promising preclinical results in glioblastoma and small-cell lung cancer models.[11,12] Notably, anti-CD47 therapy enhances phagocytic activity in both M1 and M2 macrophages, with greater efficacy observed in M1-polarized cells. Reprogramming TAMs has the potential to augment existing treatments such as chemotherapy and immune checkpoint inhibitors by reversing immunosuppression and boosting antitumor immunity. Combination strategies that simultaneously target multiple immunosuppressive pathways have demonstrated synergistic effects, including enhanced tumoricidal activity and improved treatment outcomes, particularly in therapy-resistant tumors.[4,13]

In this study, we explored the therapeutic potential of combining TAM reprogramming with anti-CD47 therapy in recurrent head and neck squamous cell carcinoma (HNSCC). HNSCC is characterized by a high recurrence rate, with approximately 50% of patients experiencing locoregional or distant recurrence, the majority of which occur within the first two years following definitive treatment.[14,15] Patients with recurrent or metastatic (R/M) disease face a particularly poor prognosis; even with platinum-based chemotherapy, the median overall survival remains 6 months or less, underscoring the urgent need for novel therapeutic strategies.[15]

Specifically, we investigated the synergistic effects of co-targeting CD47 and EphA3, a receptor tyrosine kinase implicated in macrophage polarization. We hypothesized that simultaneous inhibition of these pathways would block immune evasion and reprogram TAMs from an M2-like, tumor-supportive phenotype to an M1-like, tumor-suppressive phenotype.

Materials and Methods

Cell Culture and Generation of Recurrent Head and Neck Cancer Cells

Human head and neck squamous cell carcinoma (HNSCC) cell lines (AMC-HN3, AMC-HN3R, HN31, HN31R) were used in this study. AMC-HN3 cells were obtained from Asan Medical Center (Seoul, Korea), and HN31 cells were generously provided by Dr. Jeffrey N. Myers (MD Anderson Cancer Center, University of Texas, Houston, TX, USA). The use of these cell lines in this study was approved by the Institutional Review Board (IRB) and Ethics Committee of Ulsan University Hospital, Republic of Korea (IRB No. NON2021-006). Cells were cultured in Dulbecco's Modified Eagle Medium (DMEM; Invitrogen, Carlsbad, CA, USA) supplemented with 10% fetal bovine serum (FBS) and 100 μg/mL penicillin/streptomycin at 37 °C in a humidified atmosphere containing 5% CO_2.

Mouse oral squamous cell carcinoma (MOC2) cells were obtained from Kerafast (Boston, MA, USA) and cultured according to the manufacturer's instructions. MOC2 and radiation-resistant MOC2R cells were maintained in a 2:1 mixture of IMDM and F12 media supplemented with 5% FBS (Fisher Scientific, Houston, TX), 1% penicillin/

streptomycin, 1% amphotericin B, 5 ng/mL EGF (Millipore), 400 ng/mL hydrocortisone, and 5 mg/mL insulin (Sigma-Aldrich). To establish radiation-resistant cells, parental cells were exposed to 35 cycles of irradiation totaling 70 Gy.[16] Resistance was validated using clonogenic survival and migration/invasion assays (Supplementary Figure S1).

Clonogenic Assay

Cells were seeded and incubated for 14 days. Colonies consisting of >50 cells were fixed with methanol and stained with crystal violet. The surviving fraction (SF) was calculated using the formula:

$$SF = (\text{number of colonies}) / (\text{number of cells seeded} \times \text{plating efficiency}).$$

RNA Interference

MOC2R cells were transfected with shRNA plasmids targeting EphA3 (sc-39935-SH) or CD47 (sc-35007-SH), both obtained from Santa Cruz Biotechnology (Dallas, TX, USA). Each plasmid pool contained three lentiviral vectors encoding 19–25 nt shRNAs with puromycin resistance markers. Transfections were performed using UltraCruz transfection reagent per manufacturer's instructions. Briefly, 1×10^5 cells per well were plated in six-well plates with antibiotic-free medium and incubated for 24 hours. Cells were transfected with 1 µg plasmid DNA and incubated at 37 °C under 5% CO_2. Gene expression levels were analyzed on days 3 and 7 post-transfection. For functional assays, anti-EphA3 monoclonal antibody (KB004; MedChemExpress), isotype control (KB243), and anti-CD47 antibody (clone MIAP410; BioXCell) were used.

Real-Time PCR

Total RNA was extracted using the PureLink™ RNA Mini Kit (Invitrogen). Real-time PCR was conducted using an ABI Prism 7500 system (Applied Biosystems), with mRNA normalized to β-actin. The primer sequences used for qRT-PCR are provided in Supplementary Table S1.

Western Blot Analysis

Cell lysates were prepared using RIPA buffer with protease/phosphatase inhibitors, followed by centrifugation. Proteins were separated by SDS-PAGE, transferred to PVDF membranes, blocked with 5% milk, and incubated with primary antibodies overnight at 4 °C. After washing with TBS-T, HRP-conjugated secondary antibodies were applied, and proteins were detected using ECL. Molecular weight markers were included or indicated on the original blots using the following prestained protein ladders: PageRuler™ Plus Prestained Protein Ladder (10–250 kDa; Thermo Scientific, Cat# 26619), PageRuler™ Prestained Protein Ladder (10–180 kDa; Thermo Scientific, Cat# 26616), Color Prestained Protein Standard, Broad Range (11–245 kDa; New England Biolabs, Cat# P7712S), and Xpert Prestained Protein Marker (10–250 kDa; GenDEPOT, Cat# P8502-050). The following antibodies were used in this study: EphA3 (sc-514209; Santa Cruz Biotechnology), CD47 (#MA5-35102; Invitrogen), β-actin (sc-47778; Santa Cruz Biotechnology), Inos (#PA1-036; Invitrogen), Arginase-1 (#PA5-29645; Invitrogen), ARID5A (#MA5-27814; Invitrogen), FOSL2 (HPA004817; Sigma-Aldrich), and DVL3 (#PA5-17482; Invitrogen).

Immunoprecipitation and Immunoblotting Analysis

Cell lysates (1 mL containing 500 µg of total protein) were pre-cleared with 5 µg of normal rabbit IgG and 10 µg of Protein A/G agarose beads (Pierce Classic IP Kit, #26146, Thermo Fisher Scientific). The beads were washed with immunoprecipitation (IP) wash buffer composed of 25 mM Tris, 150 mM NaCl, 1 mM EDTA, 1% NP-40, and 5% glycerol (pH 7.4). After the final wash, the pre-cleared lysates were incubated overnight at 4 °C with constant rotation in the presence of 5 µg of specific antibodies against EphA3 (sc-514209; Santa Cruz Biotechnology), Dvl3 (#PA5-17482; Invitrogen), or normal rabbit IgG (sc-2027; Santa Cruz Biotechnology) as a control. The next day, Protein A/G agarose beads were added to the mixture and incubated for 1 additional hour at 4 °C. The resulting immunoprecipitates were washed thoroughly with a buffer containing 0.5% Triton X-100 to remove non-specific binding. For immunoblotting, 10 µg of total protein from whole-cell extracts was separated via SDS-PAGE and transferred onto nitrocellulose (NC)

membranes. Membranes were blocked in 5% non-fat dry milk and then incubated sequentially with primary and HRP-conjugated secondary antibodies. Protein bands were visualized using an enhanced chemiluminescence (ECL) detection system.

Macrophage Preparation and Polarization

Bone marrow-derived macrophages (BMDMs) were generated by flushing tibiae and femurs from C57BL/6 mice and resuspending the cells in RPMI 1640 medium supplemented with 10% fetal bovine serum (FBS), 1% penicillin/streptomycin (P/S), and 20 ng/mL mouse macrophage colony-stimulating factor (M-CSF; Roche, Mannheim, Germany). Cells were plated in six-well plates, and the medium was replaced every 3 days with fresh RPMI 1640 containing the same supplements until undifferentiated M0 macrophages were obtained.

Macrophage polarization was then induced. M1 macrophages were generated by stimulating M0 macrophages with lipopolysaccharide (LPS, 100 ng/mL) and interferon-γ (IFN-γ, 100 U/mL) for 24 hours. M2 macrophages were induced by treating M0 macrophages with interleukin-4 (IL-4, 20 ng/mL) for 24 hours.

To investigate the effects of CD47 and/or EphA3 inhibition on M2 polarization, macrophages were first polarized with IL-4 (20 ng/mL, 24 h), followed by pretreatment with anti-CD47 (clone MIAP301; BioXCell) and/or anti-EphA3 (KB004; MedChemExpress) antibodies for 1 hour.

Phagocytosis Assay

Bone marrow-derived macrophages (BMDMs) were isolated from C57BL/6 mice and cultured for 7 days in RPMI 1640 medium supplemented with 20 ng/mL macrophage colony-stimulating factor (M-CSF; Peprotech, Rocky Hill, CT, USA). During this period, the culture medium was replaced regularly with fresh medium containing M-CSF. After differentiation, adherent macrophages were harvested for downstream experiments.

For phagocytosis assays, BMDMs were co-cultured with either APC^+ or CFSE-labeled tumor cells at a 1:3 (macrophage:tumor cell) ratio in serum-free medium at 37 °C for 4 hours. After incubation, cells were collected and stained with anti-F4/80 antibody (eBioscience, San Diego, CA, USA) for macrophage identification by flow cytometry.

In inhibitor experiments, M2 macrophages were first polarized by IL-4 treatment (20 ng/mL, 24 h), followed by pretreatment with anti-CD47 and/or anti-EphA3 antibodies for 1 hour prior to co-culture. The phagocytic index was calculated using the following formula:

$$\text{Phagocytosis rate (\%)} = (\text{F4/80}^+\ \text{CFSE}^+ \text{ cells / total F4/80}^+ \text{ cells}) \times 100.$$

Immunofluorescence Staining (Cell-Based)

Cells (1×10^4 per well) were seeded onto poly-D-lysine-coated glass coverslips (Sigma-Aldrich) in 24-well plates. After serum starvation, cells were treated for 24 hours with various types of conditioned media (CM), including CM derived from M2 macrophages or in vitro-induced M2-like TAMs. Treatments were divided into four groups: (a) isotype control, (b) anti-CD47 antibody (10 μg/mL), (c) anti-EphA3 antibody (10 μg/mL), and (d) a combination of both antibodies.

Following treatment, cells were fixed with 4% paraformaldehyde and stained with primary antibodies: mouse anti-mouse ARID5A (Invitrogen) and rabbit anti-mouse FOSL2 (Sigma-Aldrich). Additional primary antibodies, including iNOS (#PA1-036), arginase-1 (#PA5-29645), ARID5A (#MA5-27814), and FOSL2 (#HPA004817), were obtained from Santa Cruz Biotechnology, Sigma-Aldrich, and Invitrogen. Fluorophore-conjugated secondary antibodies included goat anti-rabbit Alexa Fluor 647 and goat anti-mouse Alexa Fluor 488. Nuclear staining was performed with DAPI (Invitrogen). Images were captured using fluorescence or confocal microscopy at 20× or 40× magnification. All Alexa Fluor-labeled antibodies were sourced from Invitrogen (Thermo Fisher, San Diego, CA, USA).

Immunofluorescence Staining (Tissue Sections)

Paraffin-embedded tissue sections were deparaffinized by incubation at 60 °C for 1 hour, followed by xylene treatment for 30 minutes. Rehydration was performed stepwise using 100%, 95%, and 70% ethanol, then isopropanol. Antigen

retrieval was conducted by heating the slides in citrate buffer for 30 minutes. After washing in PBS, slides were blocked with 5% bovine serum albumin (BSA) at room temperature for 1 hour.

Slides were then incubated overnight at 4 °C with primary antibodies against β-catenin, followed by three PBS washes. Alexa Fluor 488-conjugated goat anti-rabbit IgG and Alexa Fluor 647-conjugated goat anti-mouse IgG were applied for 1 hour at room temperature. After three additional washes, DAPI was applied for 15 minutes to stain nuclei. Slides were washed again with PBS and mounted with DAKO tissue mounting medium (Agilent, CA, USA). Images were acquired using a Zeiss LSM 710 confocal microscope and processed with Zen software.

Heatmap, Hierarchical Clustering, and Differentially Expressed Gene Analysis

Gene expression data were analyzed using ExDEGA software (version 1.2.1.0; EBIOGEN Inc., Seoul, Korea). Differentially expressed genes were identified using a threshold of gene count > 2 and $p < 0.05$. Hierarchical clustering (HCL) analysis was performed using the MeV software package. To identify pathway-level changes following EphA3 inhibition, top DEGs were further categorized based on their biological relevance to NF-κB/TNF-associated inflammatory signaling and STAT1/IFNγ signaling pathways. Representative genes from each pathway were selected and are presented in Supplemental Tables S2 and S3.

Flow Cytometry Analysis

To assess tumor-infiltrating macrophages, tumor tissues were finely minced and digested in RPMI medium containing 1 mg/mL Collagenase Type IV (Sigma-Aldrich) and 1 mg/mL DNase I (Roche) at 37 °C for 1 hour, with mechanical disruption by pipetting every 15 minutes. After enzymatic digestion, EDTA was added to a final concentration of 10 mM for 5 minutes. The resulting cell suspension was passed through a 70 μm cell strainer to obtain single-cell suspensions.

To block non-specific Fc receptor binding, cells were incubated on ice for 30 minutes with 1% Fc receptor blocking antibody (clone 2.4G2; BD Pharmingen). Cells were then washed with PBS containing 0.5% bovine serum albumin (BSA) and incubated with fluorochrome-conjugated primary antibodies at 4 °C for 30 minutes. After staining, cells were washed three times with PBS containing 0.5% BSA.

For surface and intracellular marker detection, the following antibodies were used at manufacturer-recommended dilutions in PBS containing 1% BSA and stained on ice for 30 minutes:

- Anti-rat CD45 FITC (Cat #553079; BD Biosciences)
- Anti-mouse F4/80 PE-Cy7 (Cat #123114; BioLegend)
- Anti-rat CD11b PerCP-Cy5.5 (Cat #550993; BD Biosciences)
- Anti-mouse iNOS-PE (Cat #12-5920-82; Invitrogen)
- Anti-mouse ARG1-APC (Cat #17-3697-82; Invitrogen)

Flow cytometric analysis was performed on a FACS Canto II flow cytometer (BD Biosciences), and data were analyzed using FlowJo software (Tree Star, Ashland, OR, USA). The gating strategy used for the identification of tumor-infiltrating macrophages is shown in Supplementary Figure S2.

Mouse Model

Six-week-old immunocompetent male C57BL/6 mice (Orient Bio Inc., Seongnam, Korea) were subcutaneously injected with 1×10^5 MOC2R cells. Once tumors reached an average volume of 50 mm^3, the mice were randomly assigned to one of four treatment groups (n = 4 per group):

(a) Isotype control,
(b) Anti-CD47 antibody (10 mg/kg, intraperitoneally [i.p.], every other day),
(c) Anti-EphA3 antibody (10 mg/kg, i.p., every other day), and
(d) Combination of anti-CD47 and anti-EphA3 antibodies (10 mg/kg each, i.p., every other day).

Treatments were administered for 4 weeks. Tumor volumes were measured with calipers and calculated using the formula:

$$\text{Volume} = (\text{length} \times \text{width}^2) \times 0.5.$$

Body weight was monitored regularly throughout the study. All animal experiments were performed in accordance with the relevant guidelines and regulations, and the study adhered to the ARRIVE (Reporting of in vivo Experiments) guidelines.

Animal Anesthesia and Euthanasia

All animal experiments were performed in accordance with relevant institutional and national guidelines for the care and use of laboratory animals, and complied with the recommendations of the American Veterinary Medical Association (AVMA) Guidelines for the Euthanasia of Animals.

Mice were anesthetized with an intraperitoneal injection of tribromoethanol (1.25% w/v, 20 μL/g body weight) prior to all surgical or invasive procedures. For terminal procedures, euthanasia was performed by CO_2 inhalation followed by cervical dislocation as a secondary physical method to ensure death. All efforts were made to minimize animal suffering and to reduce the number of animals used.

Ethical Approval

All animal experiments were reviewed and approved by the Institutional Animal Care and Use Committee (IACUC) of Ulsan University Hospital, Republic of Korea (Approval No. A-241219-02). All procedures were conducted in accordance with the institutional guidelines and relevant national regulations for animal research.

Immunohistochemical Analysis

Immunohistochemical (IHC) staining was performed on paired pre- and post-treatment tissue samples from 11 patients with laryngeal cancer who experienced recurrence following radiation therapy. Representative tumor regions, including the invasive front, were identified under light microscopy and selected for construction of tissue microarrays (TMAs), using two validated cores per case.

Formalin-fixed, paraffin-embedded tissue sections (4 μm thick) were deparaffinized, rehydrated, and subjected to heat-induced antigen retrieval in 0.01 M citrate buffer (pH 6.0) at 95 °C for 60 minutes. Endogenous peroxidase activity was blocked using 3% hydrogen peroxide for 15 minutes, followed by PBS washing. Slides were then incubated with a universal blocking reagent (1× Universal Blocking Agent; Power Block™, BioGenex) for 30 minutes at room temperature, followed by overnight incubation at 4 °C with anti-CD47 antibody (1:100; Invitrogen). The next day, slides were incubated with Dako REAL™ EnVision™ secondary reagent for 30 minutes, followed by visualization using DAB chromogen for 15 minutes. Sections were counterstained with Mayer's hematoxylin, dehydrated through graded alcohols, and mounted.

Immunostaining was independently evaluated by two blinded observers. Staining intensity was assessed using the immunoreactive score (IRS) system: 0 = negative, 1 = weak, 2 = moderate, 3 = strong. For statistical analysis, cases were dichotomized into negative (score 0) and positive (scores 1–3) groups. Differences in staining positivity between groups were analyzed using two-sided Fisher's exact test. P value of < 0.05 was considered statistically significant. The distribution of CD47-positive and CD47-negative cases is summarized in Supplementary Figure S3.

Hematological Analysis for Anemia Assessment

To evaluate treatment-induced anemia, peripheral blood was collected from mice at the terminal endpoint via cardiac puncture under deep anesthesia and immediately transferred into K_2EDTA-coated microtubes. All hematological analyses were performed within 30 minutes of collection.

Red blood cell (RBC) counts were determined manually using a Neubauer improved hemocytometer (Paul Marienfeld GmbH & Co. KG, Lauda-Königshofen, Germany). Whole blood was diluted 1:200 in isotonic RBC diluent,

loaded into the counting chamber, and allowed to sediment for 3–5 minutes prior to enumeration under a light microscope at 400× magnification. RBC counts were expressed as $\times 10^6$ cells/μL.

Hemoglobin (Hb) concentrations were measured using a portable point-of-care hemoglobin analyzer (Mission Hb; ACON Laboratories, San Diego, CA, USA) according to the manufacturer's instructions. Briefly, 10 μL of whole blood was applied to a disposable test strip and the Hb concentration was automatically displayed in g/dL within 10 seconds.

Hematocrit (HCT) was determined by the standard microhematocrit centrifugation method. Whole blood was loaded into hematocrit capillary tubes (Hirschmann Laborgeräte GmbH & Co. KG, Eberstadt, Germany) to approximately three-quarters capacity, sealed with critoseal at one end, and centrifuged at 12,000 × *g* for 5 minutes. HCT (%) was calculated as follows:

$$\text{HCT (\%)} = (\text{height of packed red blood cell column} / \text{total height of blood column}) \times 100$$

All three parameters — RBC count, Hb concentration, and HCT — were used collectively to evaluate anemia across treatment groups. Statistical comparisons were performed using one-way ANOVA followed by Tukey's multiple comparison test. Data are presented as mean ± SEM, and statistical significance was set at $p < 0.05$. The hematological data generated using these methods are presented in Supplementary Figure S4.[17–19]

Statistical Analysis

All statistical analyses were performed using GraphPad Prism version 8.0 (GraphPad Software, San Diego, CA, USA). Comparisons between two groups were conducted using Student's *t*-test. For comparisons involving more than two groups, one-way analysis of variance (ANOVA) followed by Tukey's post hoc test was applied. For categorical analysis of immunostaining data, immunoreactive score (IRS) results were dichotomized into negative (IRS 0) and positive (IRS 1–3) groups, and differences between groups were analyzed using a two-sided Fisher's exact test. Data are presented as mean ± standard error of the mean (SEM). A P value ≤ 0.05 was considered statistically significant.

Results

CD47 and EphA3 Expression in Radioresistant Head and Neck Cancer Models

We previously demonstrated that the expression levels of EphA3 and CD47 are elevated in radioresistant head and neck cancer (HNC) cell lines.[20–22] Consistent with these findings, we confirmed that radioresistant HNC cell lines exhibited increased CD47 and EphA3 expression compared to their parental counterparts.

Flow cytometry analysis revealed upregulated surface CD47 expression in multiple radioresistant cell lines, including HN3R, HN31R, and MOC2R, relative to their parental lines (Figure 1A). This was further validated by RT-PCR and Western blot analysis, which demonstrated significantly higher mRNA and protein levels of CD47 and EphA3 in HN31R, HN3R, and MOC2R cells (Figure 1B and C).

To assess clinical relevance, CD47 expression was evaluated in paired pre- and post-radiation tumor samples from patients using immunohistochemistry (IHC) (Figure 1D). Notably, increased CD47 expression was observed in 7 of 11 recurrent tumor specimens following radiation therapy, and the distribution of CD47-positive and CD47-negative cases in paired primary and recurrent tumors is summarized in Supplementary Figure S3. In line with our previous findings, EphA3 expression was also elevated in post-radiation recurrent tumors compared to pretreatment samples.[20]

Combination Treatment with CD47 and EphA3 Antibodies Enhances Phagocytosis and Reduces Tumor Cell Survival in vitro

To investigate the impact of CD47 and EphA3 blockade on macrophage-mediated phagocytosis and tumor cell survival, CFSE-labeled MOC2R cells—characterized by radio resistant and aggressive behavior (Supplementary Figure S1)—were co-cultured with bone marrow-derived macrophages. Cells were treated with anti-CD47, anti-EphA3, a combination of both antibodies, or an IgG isotype control. Phagocytosis was assessed by immunofluorescence staining and flow cytometry, identifying phagocytic macrophages as dual-positive for F4/80 and CFSE (Figure 2A).

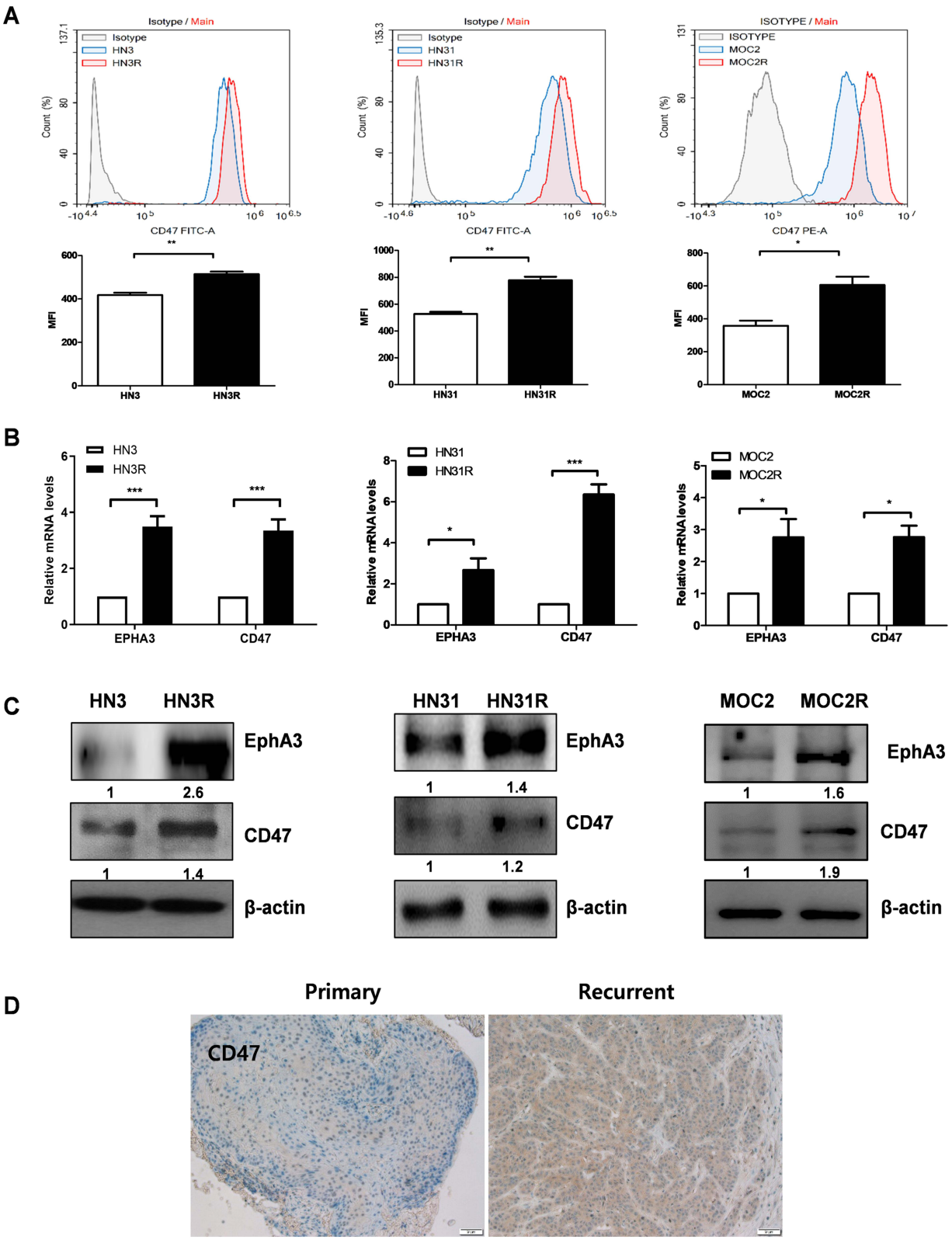

Figure 1 CD47 and EphA3 expressions in radioresistant head and neck cancer cell line. (**A**) The expression levels of CD47 in parent and radioresistant HNC cell lines were calculated by Flow cytometry. (**B**) RT-PCR measured EphA3 and CD47 mRNA levels in various parent and radioresistant HNC cell lines. (**C**) EphA3 and CD47 protein levels in parent and radioresistant HNC cell lines were determined by Western blot analysis. The protein expression levels were quantified and compared to β-actin as a loading control. (**D**) Assessment of CD47 expression in primary laryngeal cancer tissues and paired recurrent tumor tissues after radiation therapy. Scale bars represent 50 μm. Values are the means ± SD (n =3). *, $P < 0.05$ **, $P < 0.01$. ***, $P < 0.001$, n.s., not significant.

https://doi.org/10.2147/OTT.S595937

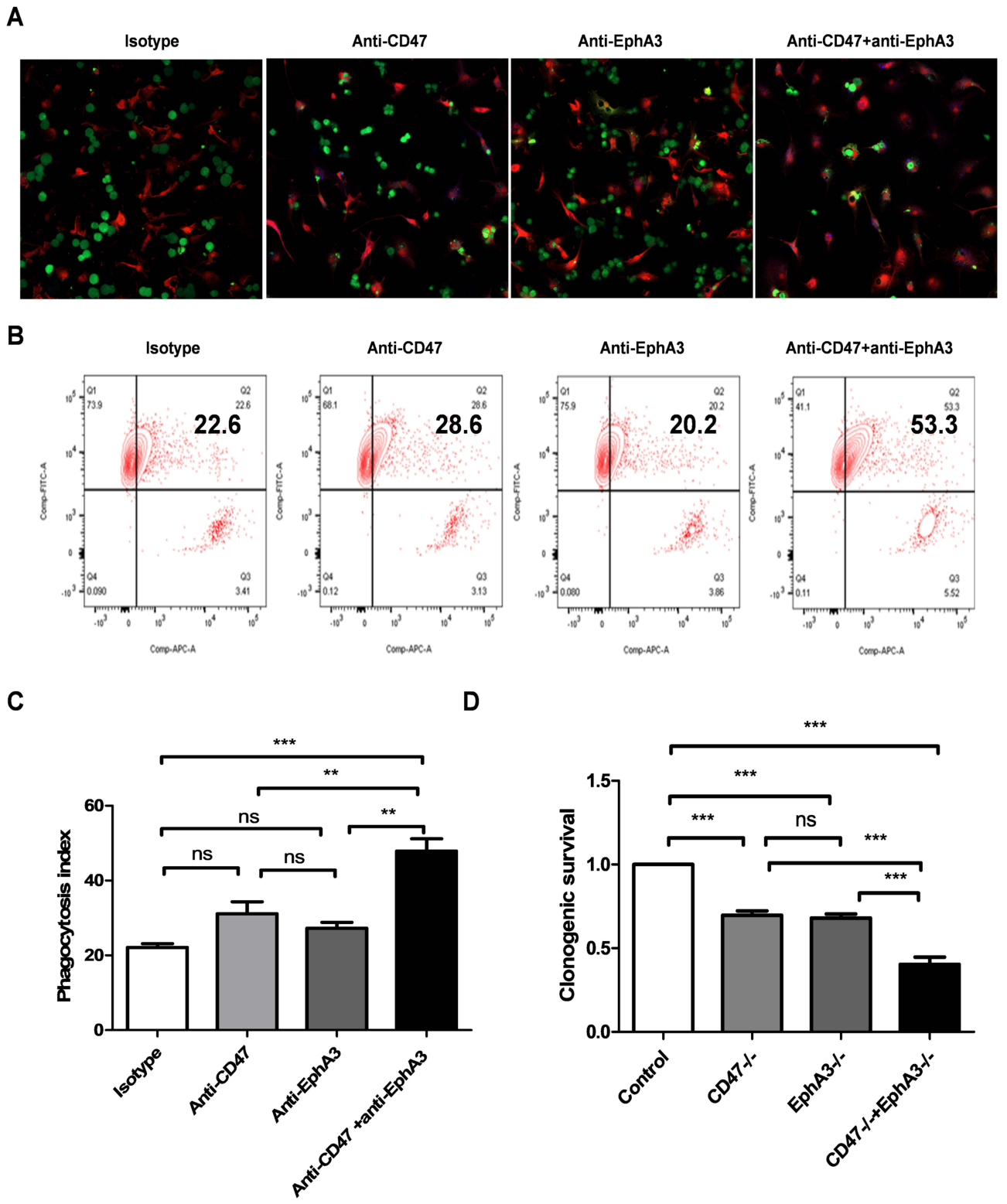

Figure 2 EphA3 antibody enhances the efficacy of CD47 antibody by increasing the phagocytosis. (**A**) An in vitro phagocytosis assay was performed using bone marrow–derived macrophages (BMDMs) co-cultured with CFSE-labeled radioresistant HNC cells (MOC2-R). Representative fluorescence images show macrophages stained for F4/80 (red) and tumor cells labeled with CFSE (green) under different treatment conditions: isotype control, anti-CD47 antibody, anti-EphA3 antibody, or the combination of both antibodies. Nuclei were counterstained with DAPI (blue). Scale bar = 50 μm. (**B**) Flow cytometry was used to demonstrate the gating strategy applied for phagocytosis quantification. (**C**) The phagocytosis index was calculated as the percentage of macrophages that had internalized tumor cells, based on flow cytometric analysis. Bars represent mean ± SD (n=3 independent experiments). (**D**) Colony formation assays were carried out using cell lines deficient in CD47 (CD47-/-), EphA3 (EphA3-/-), and a double knockout for both genes (CD47-/-/EphA3-/-). Colonies were quantified after a 14-day incubation period to assess the impact of these genetic modifications on the clonogenic potential of the cells. Statistical significance is indicated as follows. Statistical analysis: ** $P < 0.01$, *** $P < 0.001$.

https://doi.org/10.2147/OTT.S595937

Quantitative analysis of phagocytosis revealed phagocytosis indices of 22.6 (isotype control), 28.6 (anti-CD47), 20.2 (anti-EphA3), and 53.3 (combination treatment) (Figure 2B). While single-agent treatment with either anti-CD47 or anti-EphA3 did not result in a statistically significant increase in phagocytosis compared to the control, the combination therapy produced a synergistic enhancement ($P < 0.01$; Figure 2C).

To further evaluate the impact on long-term tumor cell viability, clonogenic assays were performed using gene-edited MOC2R cells: CD47 knockout ($CD47^{-/-}$), EphA3 knockout ($EphA3^{-/-}$), and double knockout ($CD47^{-/-}/EphA3^{-/-}$). After 14 days, colony numbers were significantly reduced in the double knockout group compared to either single knockout or control cells ($P < 0.0001$; Figure 2D), indicating a strong impairment in clonogenic potential. These results suggest that EphA3 inhibition enhances the therapeutic efficacy of CD47 blockade by synergistically promoting macrophage-mediated phagocytosis and reducing tumor cell survival in vitro.

Dual Blockade of CD47 and EphA3 Reprograms Macrophages from an M2 to an M1 Phenotype

To investigate the mechanisms underlying the enhanced phagocytosis and tumor cell death observed with dual CD47 and EphA3 blockade, mRNA sequencing was performed. Heatmap analysis revealed that inhibition of EphA3—either alone or in combination with CD47 blockade—promoted macrophage repolarization toward an M1-like phenotype (Figure 3A). To further characterize the transcriptomic response to EphA3 inhibition, top differentially expressed genes (DEGs) were identified (Table S2). Pathway-level analysis showed a trend toward upregulation of NF-κB/TNF-associated inflammatory genes and STAT1/IFNγ signaling-related genes following EphA3 inhibition (Table S3).

Consistent with these transcriptomic findings, quantitative real-time PCR demonstrated significant upregulation of M1-associated markers (*CD86* and *TNF-α*) and concomitant downregulation of M2-associated markers (*CD206* and *ARG1*) following 24 hours of culture under EphA3-inhibited conditions (Figure 3B). To further confirm this phenotypic shift at the protein level, immunofluorescence staining and Western blot analysis were performed after 48 hours of treatment. Macrophages treated with the combination of anti-CD47 and anti-EphA3 antibodies exhibited increased expression of inducible nitric oxide synthase (iNOS), a canonical M1 marker, and decreased expression of the M2 marker arginase-1 (ARG1) (Figure 3C and D). Collectively, these results demonstrate that dual targeting of CD47 and EphA3 effectively reprograms macrophages from an immunosuppressive M2 phenotype to a pro-inflammatory M1 phenotype, contributing to enhanced anti-tumor immune responses.

Dual Blockade of CD47 and EphA3 Enhances Antitumor Efficacy by Increasing Tumor-Infiltrating M1 Macrophages in an in vivo Mouse Model

The antitumor efficacy of dual CD47 and EphA3 blockade was evaluated using a syngeneic MOC2R tumor-bearing mouse model. Mice were randomly assigned to one of four treatment groups: isotype control, anti-CD47 alone, anti-EphA3 alone, or the combination of anti-CD47 and anti-EphA3 antibodies. Tumor volumes were measured every two days during the treatment period. On day 24, the mice were sacrificed, and both tumor volume and weight were recorded.

Combination treatment resulted in a significant reduction in tumor volume and weight compared to either monotherapy or the isotype control (Figure 4A-C). No significant differences in body weight were observed among the treatment groups during the treatment period. At the terminal endpoint, anti-CD47 monotherapy significantly reduced RBC count, hemoglobin concentration, and hematocrit relative to the isotype control. These decreases were not observed in the combination group (Supplementary Figure S4). Flow cytometry analysis of tumor tissues revealed increased infiltration of $CD45^{+}CD11b^{+}F4/80^{+}$ macrophages in the combination group (17.5%) compared to the isotype control (5.78%), anti-CD47 (13.2%), and anti-EphA3 (14.7%) groups. Within this macrophage population, the proportion of $iNOS^{+}$ M1-like tumor-associated macrophages increased from 16.7% (isotype) to 39.8% (combination treatment), while $Arg\text{-}1^{+}$ M2-like macrophages decreased from 35.6% to 18.1% (Figure 4D and E; Supplementary Figure S2). We additionally performed flow cytometric analysis of tumor-infiltrating $CD8^{+}$ T cells and observed a trend toward increased $CD8^{+}$ T-cell infiltration in the combination treatment group; however, this difference did not reach statistical significance (Supplementary Figure S5).

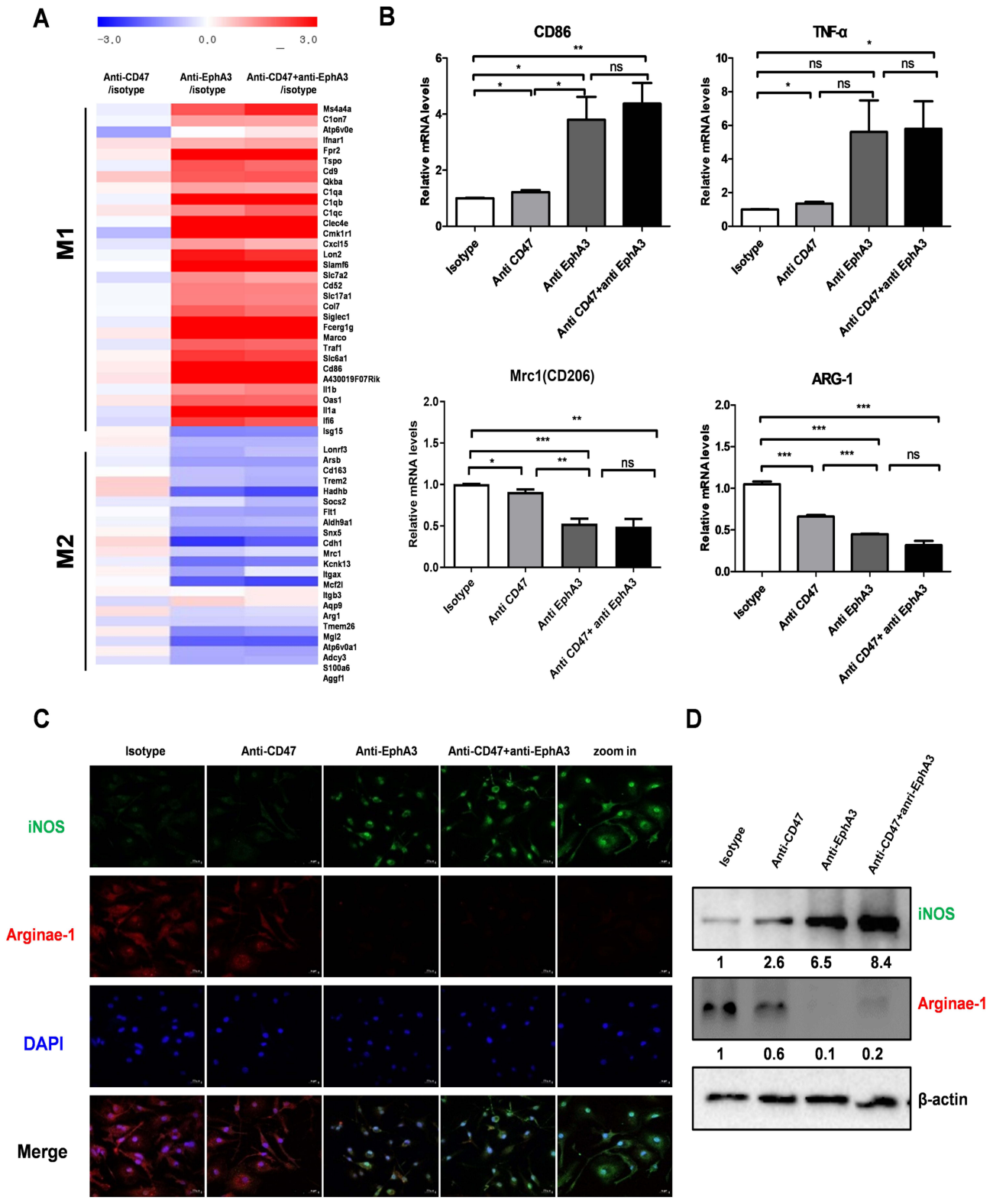

Figure 3 EphA3 blockade reprograms tumor-associated macrophages from an M2-like to M1-like phenotype. (**A**) RNA sequencing was performed to assess differential expression of M1 and M2 macrophage polarization markers in BMDMs following 24-hour treatment with isotype control, anti-CD47 antibody, anti-EphA3 antibody, or the combination of both antibodies. (**B**) Quantitative RT-PCR was conducted to validate the expression of representative M1 and M2 markers in macrophages treated as described above. (**C**) Immunofluorescence staining was carried out to visualize iNOS (green) and Arginase-1 (red) expression in macrophages treated for 48 hours. Nuclei were counterstained with DAPI (blue). (**D**) Western blot analysis was used to measure iNOS and Arg-1 protein levels in treated macrophages after 48 hours. β-actin served as a loading control. Statistical analysis was performed using one-way ANOVA. *$P < 0.05$, ** $P < 0.01$, *** $P < 0.001$.
Abbreviation: ns, not significant.

https://doi.org/10.2147/OTT.S595937

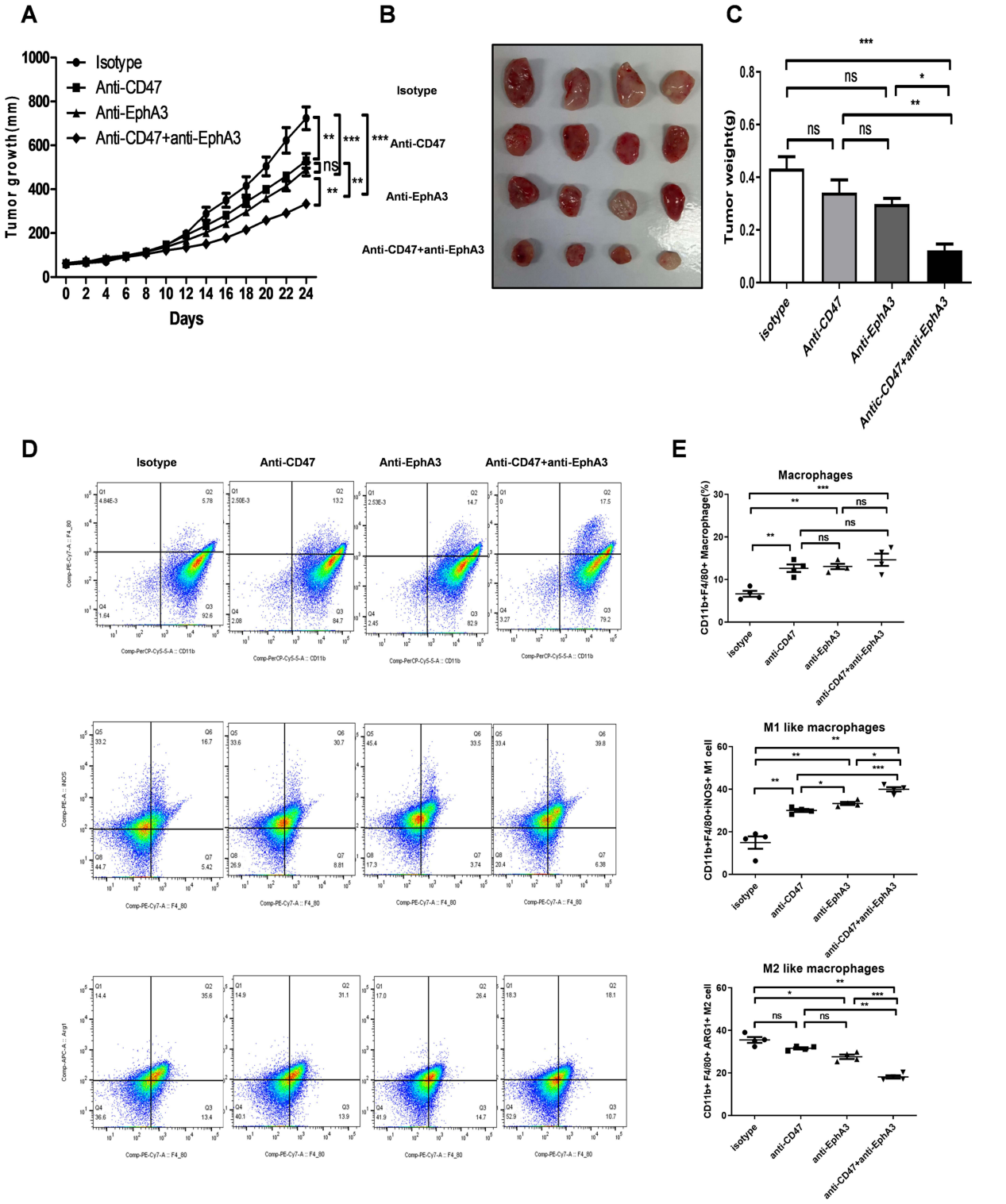

Figure 4 Dual blockade of EphA3 and CD47 enhances anti-tumor efficacy in vivo and increases infiltration of pro-inflammatory macrophages. (**A**) Syngeneic C57BL/6 mice bearing MOC2-R tumors were treated with isotype IgG, anti-CD47 antibody, anti-EphA3 antibody, or both antibodies. Tumor volumes were measured regularly to generate growth curves (n = 4 mice per group). (**B**) Representative images of tumors excised from each treatment group were taken to compare gross morphology. (**C**) Tumor volumes and weights were recorded at the endpoint of the experiment on day 24. (**D**) Flow cytometry was performed on tumor single-cell suspensions to quantify tumor-associated macrophage subsets. TAMs (Tumor-associated macrophages) were gated as $CD45^+CD11b^+F4/80^+$ cells and further analyzed for expression of M1 (iNOS+) and M2 markers (Arg1 +). (**E**) Flow cytometry data were used to quantify the proportion of M1-like and M2-like TAMs in each treatment group. Statistical analysis was performed using two-way ANOVA for the tumor growth curves in panel A and one-way ANOVA for the group comparisons in panels C and E. * $P < 0.05$, ** $P < 0.01$, *** $P < 0.001$.

Abbreviation: ns, not significant.

These results indicate that dual blockade of CD47 and EphA3 enhances antitumor immunity in vivo by promoting macrophage repolarization from an M2-like immunosuppressive state to a pro-inflammatory M1-like phenotype.

Dual Blockade of CD47 and EphA3 Reprograms Tumor Associated Macrophages (TAMs) via Modulation of the β-Catenin/FOSL2/ARID5A Signaling Axis

Although our previous findings demonstrated that EphA3 contributes to antitumor immunity by promoting macrophage reprogramming, the specific molecular pathways involved remained unclear. Members of the Eph receptor family, such as EphA2, are known to modulate Wnt/β-catenin signaling by interacting with components like Dishevelled 2 (Dvl2), which recruits Axin1 to the plasma membrane.[23] Given the structural similarity among Eph receptors, we hypothesized that EphA3 may similarly interact with the Wnt/β-catenin pathway. Regarding the reprogramming of tumor-associated macrophages by targeting the β-catenin/FOSL2/ARID5A signaling pathway,[24] to explore this hypothesis, we examined the expression of EphA3 and β-catenin in M1- and M2-polarized TAMs. Both proteins were found to be upregulated in M2 macrophages (Figure 5A). Co-immunoprecipitation (co-IP) analysis in bone marrow-derived macrophage (BMDM)-derived M2 cells revealed a physical interaction between endogenous EphA3 and Dishevelled 3 (Dvl3) (Figure 5B and C), supporting EphA3's involvement in Wnt signaling in macrophages. To further investigate the underlying mechanisms, RNA sequencing was performed. Heatmap analysis demonstrated that EphA3 inhibition resulted in downregulation of *Dvl3* and *FOSL2*, and upregulation of *ARID5A* (Figure 5D). Given these transcriptional changes, we hypothesized that EphA3 may drive M2 polarization through Dvl3-mediated activation of β-catenin, which subsequently regulates downstream effectors such as FOSL2 and ARID5A.

To validate this mechanism, we examined protein expression following EphA3 or combined EphA3 and CD47 blockade. Western blot analysis showed that dual blockade significantly reduced the levels of Dvl3 and β-catenin in M2 macrophages (Figure 5E). Immunofluorescence staining further confirmed that ARID5A expression was increased, while FOSL2 expression was decreased in response to the combination therapy (Figure 5F). These findings were corroborated at the protein level by Western blotting (Figure 5G).

Taken together, these results suggest that EphA3 promotes an M2-like immunosuppressive phenotype in TAMs by activating the β-catenin/FOSL2/ARID5A signaling axis. Dual blockade of EphA3 and CD47 not only enhances phagocytosis but also reprograms TAMs toward an M1-like, pro-inflammatory phenotype, thereby potentiating antitumor immunity.

To conceptualize this mechanism, we constructed a schematic model (Figure 6). In this model, EphA3 facilitates M2 polarization by engaging Dvl3, leading to β-catenin stabilization and nuclear translocation, which in turn upregulates FOSL2 and suppresses ARID5A expression. Inhibition of EphA3 disrupts this pathway, resulting in decreased FOSL2 and increased ARID5A expression, favoring M1 polarization. Concurrently, CD47 blockade relieves the "don't eat me" signal via SIRPα inhibition, promoting macrophage-mediated phagocytosis. The combined targeting of EphA3 and CD47 thus cooperatively reprograms TAMs toward a tumoricidal, pro-inflammatory M1 phenotype.

Discussion

In this study, we demonstrate that dual targeting of EphA3 and CD47 synergistically enhances anti-tumor immunity in radioresistant head and neck cancer (HNC). EphA3 and CD47 were found to be co-upregulated in radioresistant HNC cell lines and recurrent tumor specimens, suggesting their cooperative involvement in therapeutic resistance. EphA3 contributes to radioresistance by promoting epithelial–mesenchymal transition (EMT) and tumor–stroma interactions,[20] while CD47 prevents phagocytic clearance by delivering a "don't eat me" signal to macrophages via SIRPα.[25] The tumor-specific expression pattern of EphA3 and the radiation-induced upregulation of CD47 underscore their potential as combinatorial immunotherapeutic targets.[26] Similarly, increased CD47 expression in post-radiation tumors may allow cancer cells to evade macrophage-mediated clearance, thereby contributing to tumor recurrence.[27] The concurrent overexpression of EphA3 and CD47 in treatment-resistant, recurrent tumors suggests a cooperative mechanism: EphA3-mediated microenvironmental remodeling and CD47-dependent immune escape may work in concert to promote tumor persistence and regrowth following therapy.

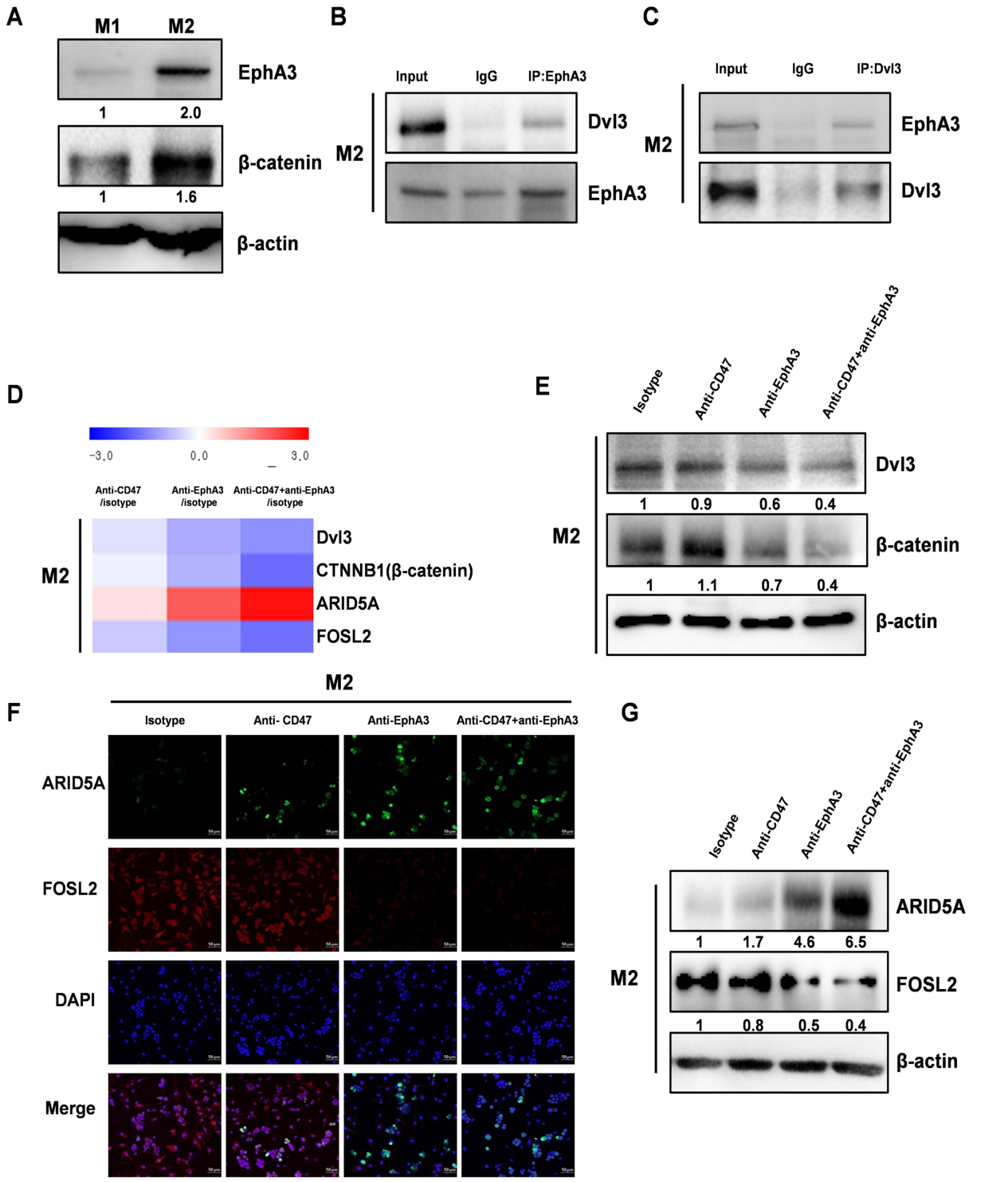

Figure 5 EphA3 inhibition in TAMs modulates the Wnt/β-catenin–FOSL2–ARID5A signaling axis to drive macrophage repolarization. (**A**) Western blotting was performed to assess baseline expression levels of EphA3 and β-catenin in BMDMs polarized to either the M1 or M2 phenotype. (**B and C**) Co-immunoprecipitation assays were conducted to detect interactions between EphA3 and Dishevelled-3 (Dvl3) in M2-polarized macrophages. (**D**) RNA-seq analysis was performed on M2-polarized BMDMs treated with anti-EphA3 and/or anti-CD47 antibodies, with a focus on the Wnt/β-catenin pathway and macrophage polarization-associated genes. (**E**) Western blotting was used to determine β-catenin and Dvl3 protein expression levels in macrophages after 24-hour treatment with the indicated antibodies. (**F**) Immunofluorescence staining of M2 macrophages was performed to assess the nuclear expression of FOSL2 (red) and ARID5A (green) after 48-hour treatment. Nuclei were counterstained with DAPI (blue). (**G**) Western blot analysis was performed to assess ARID5A and FOSL2 protein expression in M2-like macrophages treated with isotype control, anti-CD47 antibody, anti-EphA3 antibody, or the combination of both antibodies. β-actin served as a loading control. Statistical analysis was performed using one-way ANOVA. *$P < 0.05$, ** $P < 0.01$, *** $P < 0.001$.

Abbreviation: ns, not significant.

https://doi.org/10.2147/OTT.S595937

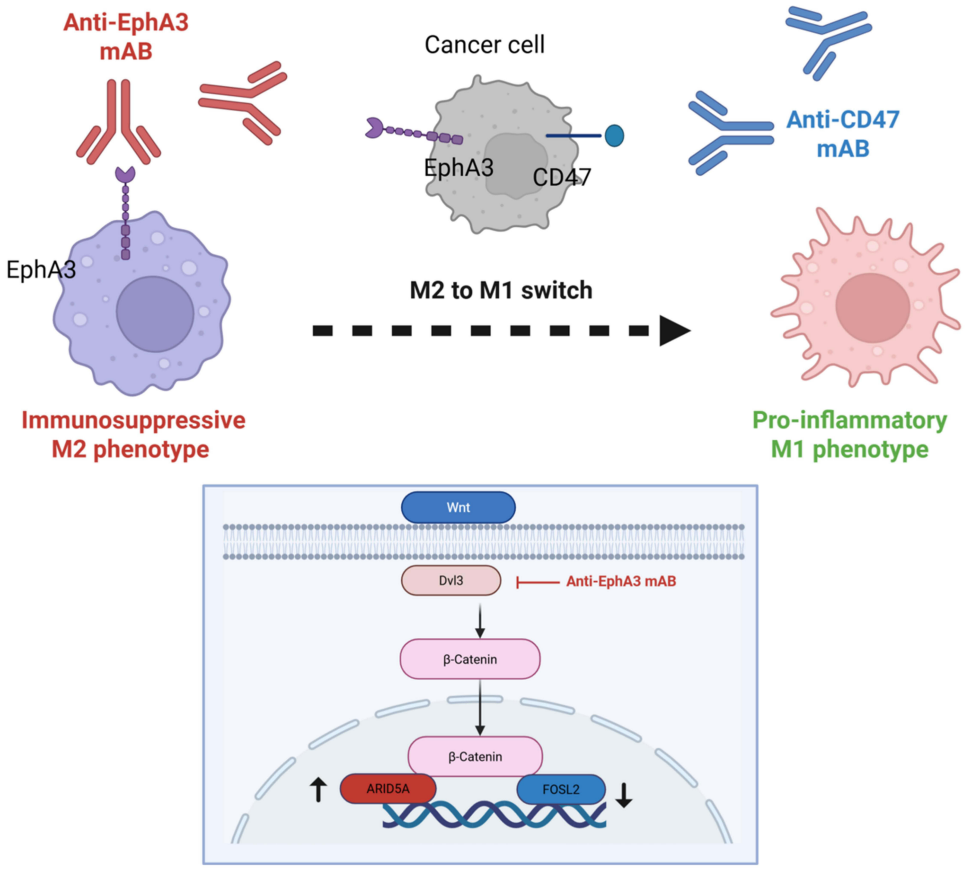

Figure 6 Schematic representation of EphA3/CD47 blockade–induced M2-to-M1 macrophage reprogramming. Anti-EphA3 monoclonal antibody (mAb) inhibits EphA3 signaling in M2-like tumor-associated macrophages, resulting in suppression of the Wnt/β-catenin signaling pathway. This effect decreases FOSL2 expression and increases ARID5A expression, promoting a phenotypic switch toward pro-inflammatory M1 macrophages. Concurrent blockade of CD47 on tumor cells with anti-CD47 mAb disrupts anti-phagocytic signaling and facilitates macrophage-mediated tumor cell clearance. Together, these actions lead to effective macrophage reprogramming and enhanced anti-tumor immunity. Created with BioRender.com.

A central finding of this study is that combined blockade of CD47 and EphA3 synergistically enhances macrophage-mediated phagocytosis and suppresses tumor cell viability in radioresistant HNC. Dual-antibody treatment more than doubled the phagocytosis index compared to control and significantly reduced clonogenic survival, indicating a supra-additive effect. CD47/SIRPα signaling is a well-characterized pathway that inhibits macrophage phagocytic activity by delivering a "don't eat me" signal to innate immune cells.[25,28] While CD47 blockade removes this inhibitory signal, its effectiveness may be limited in tumors with an immunosuppressive microenvironment, where tumor-associated macrophages (TAMs) are often polarized toward an M2-like, anti-inflammatory phenotype with reduced phagocytic potential.[10,29–32] Our data suggest that EphA3 inhibition reprograms TAMs toward a pro-inflammatory, M1-like state, thereby complementing the effects of CD47 blockade.

In this context, dual targeting exerts a two-pronged effect: CD47 inhibition permits phagocytosis, while EphA3 blockade actively drives macrophage activation toward a tumoricidal phenotype. This combined strategy leads to enhanced engulfment of tumor cells and impaired tumor colony formation. These findings underscore a broader concept—effective macrophage-based immunotherapy may require not only releasing inhibitory checkpoints but also inducing a favorable functional state. Consistent with this, multi-modal approaches targeting both the immune effector cell and the tumor microenvironment have shown promise. For example, combining CD47 blockade with PD-1/PD-L1 inhibitors improves tumor control in HNC compared to monotherapies.[27] Our study builds on this strategy by identifying EphA3 as a TAM-regulating receptor whose inhibition enhances the efficacy of anti-phagocytic checkpoint blockade, thereby simultaneously modulating both macrophage function and the tumor microenvironment.

https://doi.org/10.2147/OTT.S595937

Our study provides novel mechanistic insight into how EphA3 inhibition reprograms TAMs from an M2- to an M1-like phenotype. Transcriptomic and proteomic analyses revealed a functional link between EphA3 signaling and the Wnt/β-catenin pathway in macrophages. Specifically, M2-polarized macrophages exhibited higher expression of both EphA3 and β-catenin compared to M1-polarized counterparts.

EphA3 appears to interact with Wnt signaling machinery, as evidenced by its physical association with Dishevelled-3 (Dvl3) in M2 TAMs and the downregulation of Dvl3 following EphA3 inhibition. Notably, blocking EphA3—particularly in combination with CD47 inhibition—led to reduced expression of β-catenin and its downstream effector FOSL2, a transcription factor associated with M2 polarization. Concurrently, expression of ARID5A, a gene linked to M1 macrophage programming, was upregulated.

This mechanistic axis aligns with recent reports indicating that Wnt/β-catenin signaling in TAMs promotes an M2 phenotype through FOSL2 induction and ARID5A suppression, and that elevated β-catenin and FOSL2 (alongside low ARID5A) are correlated with poor prognosis in cancer.[24] By disrupting the β-catenin–FOSL2 signaling axis, EphA3 blockade effectively reprograms TAMs toward an M1-like phenotype. Our data suggest that EphA3 functions as an upstream modulator sustaining the M2-like, pro-tumoral state of macrophages, likely by facilitating Wnt/β-catenin signaling. When EphA3 is inhibited, this signaling loop is dismantled—Dvl3 and β-catenin levels decline, FOSL2-driven M2 gene expression is reduced, and suppression of M1-associated genes such as *ARID5A* is lifted—resulting in macrophages more capable of mounting anti-tumor responses. To our knowledge, this is the first demonstration of an Eph receptor regulating macrophage polarization. While prior studies have shown that EphA2 interacts with Wnt signaling in cancer cells,[23] our findings extend this crosstalk to immune cells.

These insights position EphA3 at a critical signaling nexus within TAMs, modulating their functional phenotype and enhancing the impact of concurrent immune checkpoint blockade, such as CD47/SIRPα inhibition. The synergy between EphA3 and CD47 targeting has significant implications for developing next-generation immunotherapies, particularly in treatment-refractory HNC and other solid tumors characterized by abundant TAM infiltration. While CD47-blocking agents (eg., magrolimab) are currently in clinical trials,[32] but their success in solid tumors may be limited by the immunosuppressive tumor microenvironment and their efficacy may be limited in solid tumors due to an immunosuppressive microenvironment enriched with M2 TAMs. Our findings suggest that adding a TAM-reprogramming agent like anti-EphA3 could enhance therapeutic outcomes by simultaneously promoting macrophage activation and relieving phagocytic inhibition.

EphA3 is an attractive target in this context, given its high expression in tumors—including stromal and immune components—and low expression in most normal adult tissues, suggesting a favorable therapeutic index. Previous preclinical studies have shown that EphA3-targeting antibodies can disrupt the tumor microenvironment and suppress tumor growth,[26] supporting its potential to "soften" tumor niches. When combined with CD47 blockade, which restores macrophage phagocytic function, this two-pronged strategy could achieve potent anti-tumor effects. Given the known erythrocyte-related hematologic toxicity associated with CD47 blockade, the hematologic findings in our study are also relevant to the therapeutic index of this combination strategy. Although anti-CD47 monotherapy reduced RBC count, hemoglobin concentration, and hematocrit, the addition of anti-EphA3 did not show a comparable decline in these parameters. Together with the absence of significant body weight changes, these findings suggest that anti-EphA3 did not aggravate the hematologic toxicity associated with anti-CD47 monotherapy in this model.

Clinically, such a strategy may be particularly valuable for patients with radioresistant or recurrent HNC, who often respond poorly to standard therapies. For instance, only ~20% of patients with recurrent/metastatic HNC respond to PD-1 inhibitors, and resistance is frequently linked to compensatory upregulation of innate immune checkpoints like CD47.[27] Our results highlight a potential novel combination immunotherapy—anti-EphA3 plus anti-CD47—that engages innate immunity to overcome resistance. Furthermore, this dual-targeting approach may extend beyond HNC, as TAM-driven immune suppression and CD47-mediated evasion are common features in multiple solid tumors, including lung, breast, and pancreatic cancers.[33]

While this study provides compelling preclinical evidence for the therapeutic potential of dual EphA3 and CD47 targeting, several limitations should be noted. First, our in vitro and in vivo experiments were primarily conducted in murine HNC models, including the MOC2-R cell line and syngeneic tumors. The generalizability of these findings to other tumor types and human patients remains to be validated. To further explore the potential source of EPHA3 expression in human HNSCC, we analyzed TCGA HNSCC bulk RNA-seq data using the CIBERSORT algorithm in

TIMER2.0 to estimate immune cell composition. In HPV-negative HNSCC, EPHA3 expression was more closely associated with the M2 macrophage-related score than with the M1 macrophage-related score, suggesting a possible link between EPHA3 expression and an M2-like macrophage-enriched microenvironment. However, because this analysis is based on bulk transcriptomic data, it does not definitively establish macrophages as the direct cellular source of EPHA3. Consistent with this limitation, although our IHC analysis revealed elevated EphA3 expression in recurrent tumors, the specific cellular source, such as tumor cells, macrophages, or stromal components, could not be determined. Future studies using co-localization approaches, such as dual immunofluorescence with macrophage markers, will be needed to determine whether EphA3 is expressed in human TAMs and whether these cells respond similarly to EphA3 inhibition. Second, although our data suggest a mechanistic link between EphA3 inhibition and modulation of the Wnt/β-catenin pathway in macrophages, the precise molecular interactions remain to be elucidated. Whether EphA3 directly stabilizes β-catenin—similar to the known interaction between EphA2 and Wnt signaling components,[23] or exerts its effects indirectly through paracrine signaling is not yet clear. Further studies may uncover additional therapeutic targets along this pathway, such as Dvl3 or β-catenin itself, that could mimic the effects of EphA3 inhibition. Third, our in vivo findings were generated in an immune-competent mouse model, which may not fully replicate the complexity of the human tumor microenvironment. While this study focused on macrophages, the contribution of other immune cell subsets, including T cells and NK cells—under dual EphA3/CD47 blockade was not explored. Comprehensive immune profiling will be necessary to better understand the broader immunological effects of this combination strategy.

Finally, future studies should evaluate the efficacy and safety of EphA3 and CD47 dual blockades in more clinically relevant models, including patient-derived xenografts (PDXs) or genetically engineered mouse models, to better reflect human tumor heterogeneity and therapeutic response.

Conclusion

Our findings establish EphA3 as a novel regulator of TAM polarization and provide preclinical evidence that dual targeting of EphA3 and CD47 reprograms macrophages, enhances phagocytosis, and suppresses tumor progression in radioresistant HNC. These results support further development of this combination approach as a promising immunotherapeutic strategy, particularly for patients with recurrent, treatment-refractory HNC.

Data Sharing Statement

The data supporting the findings of this study are available from the corresponding author upon reasonable request.

Ethics Approval and Consent to Participate

All animal experiments were reviewed and approved by the Institutional Animal Care and Use Committee (IACUC) of Ulsan University Hospital, Republic of Korea (Approval No. A-241219-02). All procedures were conducted in accordance with the institutional guidelines and relevant national regulations for animal research.

Author Contributions

All authors made a significant contribution to the work reported, whether that is in the conception, study design, execution, acquisition of data, analysis and interpretation, or in all these areas; took part in drafting, revising or critically reviewing the article; gave final approval of the version to be published; have agreed on the journal to which the article has been submitted; and agree to be accountable for all aspects of the work.

Funding

This work was supported by the National Research Foundation (NRF) grants NRF-2023R1A2C1006630, NRF-RS-2023-NR076796, NRF-2023R1A2C2004057 and NRF-RS-2022-NR071235.

Disclosure

The authors declare no competing interests in this work.

References

1. Zhou K, Cheng T, Zhan J. et al. Targeting tumor-associated macrophages in the tumor microenvironment. *Oncol Lett*. 2020;20:234. doi:10.3892/ol.2020.12097
2. Liu L, Chen G, Gong S, Huang R, Fan C. Targeting tumor-associated macrophage: an adjuvant strategy for lung cancer therapy. *Front Immunol*. 2023;14:1274547. doi:10.3389/fimmu.2023.1274547
3. Shettigar A, Salunke R, Modi D, Mukherjee N. Targeting molecular cross-talk between tumor cells and tumor associated macrophage as therapeutic strategy in triple negative breast cancer. *Int Immunopharmacol*. 2023;119:110250. doi:10.1016/j.intimp.2023.110250
4. Shao S, Miao H, Ma W. Unraveling the enigma of tumor-associated macrophages: challenges, innovations, and the path to therapeutic breakthroughs. *Front Immunol*. 2023;14:1295684. doi:10.3389/fimmu.2023.1295684
5. Larionova I, Cherdyntseva N, Liu T, Patysheva M, Rakina M, Kzhyshkowska J. Interaction of tumor-associated macrophages and cancer chemotherapy. *Oncoimmunology*. 2019;8(7):1596004. doi:10.1080/2162402X.2019.1596004
6. Yu T, Gan S, Zhu Q, et al. Modulation of M2 macrophage polarization by the crosstalk between Stat6 and Trim24. *Nat Commun*. 2019;10:4353. doi:10.1038/s41467-019-12384-2
7. Li M, Li M, Yang Y, et al. Remodeling tumor immune microenvironment via targeted blockade of PI3K-γ and CSF-1/CSF-1R pathways in tumor associated macrophages for pancreatic cancer therapy. *J Control Release*. 2020;321:23–35. doi:10.1016/j.jconrel.2020.02.011
8. Hagemann T, Biswas SK, Lawrence T, Sica A, Lewis CE. Regulation of macrophage function in tumors: the multifaceted role of NF-kappaB. *Blood*. 2009;113:3139–3146. doi:10.1182/blood-2008-12-172825
9. Zhang M, Hutter G, Kahn SA, et al. Anti-CD47 treatment stimulates phagocytosis of glioblastoma by M1 and M2 polarized macrophages and promotes M1 polarized macrophages in vivo. *PLoS One*. 2016;11:e0153550. doi:10.1371/journal.pone.0153550
10. Zhang SY, Song XY, Li Y, Ye LL, Zhou Q, Yang WB. Tumor-associated macrophages: a promising target for a cancer immunotherapeutic strategy. *Pharmacol Res*. 2020;161:105111. doi:10.1016/j.phrs.2020.105111
11. Veillette A, Chen J. SIRPα-CD47 immune checkpoint blockade in anticancer therapy. *Trends Immunol*. 2018;39:173–184. doi:10.1016/j.it.2017.12.005
12. Pai S, Bamodu OA, Lin YK, et al. CD47-SIRPα signaling induces epithelial-mesenchymal transition and cancer stemness and links to a poor prognosis in patients with oral squamous cell carcinoma. *Cells*. 2019;8. doi:10.3390/cells8121658
13. Brady RV, Thamm DH. Tumor-associated macrophages: prognostic and therapeutic targets for cancer in humans and dogs. *Front Immunol*. 2023;14:1176807. doi:10.3389/fimmu.2023.1176807
14. Matsuo S, Habu N, Hirose H, et al. Interval to recurrence affects survival in recurrent head and neck squamous cell carcinoma. *Cancer Diagn Progn*. 2024;4(5):549–556.
15. Haring CT, Kana LA, Dermody SM, et al. Patterns of recurrence in head and neck squamous cell carcinoma to inform personalized surveillance protocols. *Cancer*. 2023;129(18):2817–2827. doi:10.1002/cncr.34823
16. Chang HW, Kim SY, Yi SL, et al. Expression of Ku80 correlates with sensitivities to radiation in cancer cell lines of the head and neck. *Oral Oncol*. 2006;42:979–986. doi:10.1016/j.oraloncology.2005.12.016
17. Lin FC, Karwan M, Saleh B, et al. IFN-γ causes aplastic anemia by altering hematopoietic stem/progenitor cell composition and disrupting lineage differentiation. *Blood*. 2024;124:3699–3708. doi:10.1182/blood-2014-01-549527
18. Handin RI, Lux SE, Stossel TP, eds.. *Blood: Principles and Practice of Hematology*. 2nd ed. Philadelphia: Lippincott Williams & Wilkins; 2003.
19. Raabe BM, Artwohl JE, Purcell JE, Lovaglio J, Fortman JD. Effects of weekly blood collection in C57BL/6 mice. *J Am Assoc Lab Anim Sci*. 2011;50:680–685.
20. Kim SH, Lee WH, Kim SW, et al. EphA3 maintains radioresistance in head and neck cancers through epithelial mesenchymal transition. *Cell Signal*. 2018;47:122–130. doi:10.1016/j.cellsig.2018.04.001
21. Kim SH, Kang BC, Seong D, et al. EPHA3 contributes to epigenetic suppression of PTEN in radioresistant head and neck cancer. *Biomolecules*. 2021;11:599. doi:10.3390/biom11040599
22. Lee WH, Kim SH, An JH, et al. Tristetraprolin regulates phagocytosis through interaction with CD47 in head and neck cancer. *Exp Ther Med*. 2022;24:541. doi:10.3892/etm.2022.11478
23. Peng Q, Chen L, Wu W, et al. EPH receptor A2 governs a feedback loop that activates Wnt/β-catenin signaling in gastric cancer. *Cell Death Dis*. 2018;9:1146. doi:10.1038/s41419-018-1164-y
24. Sarode P, Zheng X, Giotopoulou GA, et al. Reprogramming of tumor-associated macrophages by targeting β-catenin/FOSL2/ARID5A signaling: a potential treatment of lung cancer. *Sci Adv*. 2020;6:eaaz6105. doi:10.1126/sciadv.aaz6105
25. Tong B, Wang M. CD47 is a novel potent immunotherapy target in human malignancies: current studies and future promises. *Future Oncol*. 2018;14:2179–2188. doi:10.2217/fon-2018-0035
26. Vail ME, Murone C, Tan A, et al. Targeting EphA3 inhibits cancer growth by disrupting the tumor stromal microenvironment. *Cancer Res*. 2014;74:4470–4481. doi:10.1158/0008-5472.CAN-14-0218
27. Siva NR, Dai J, Chardon-Robles J, et al. Anti-CD47 and anti-PDL1 immunotherapy synergize for anti-tumor activity in preclinical models of head and neck cancer. *Int J Radiat Oncol Biol Phys*. 2024;118:e85. doi:10.1016/j.ijrobp.2024.01.189
28. Hendriks M, Ploeg EM, Koopmans I, et al. Bispecific antibody approach for EGFR-directed blockade of the CD47-SIRPα "don't eat me" immune checkpoint promotes neutrophil-mediated trogoptosis and enhances antigen cross-presentation. *Oncoimmunology*. 2020;9:1824323. doi:10.1080/2162402X.2020.1824323
29. Li C, Xu X, Wei S, Jiang P, Xue L, Wang J. Tumor-associated macrophages: potential therapeutic strategies and future prospects in cancer. *J Immunother Cancer*. 2021;9:e001341. doi:10.1136/jitc-2020-001341
30. Guan L, Xu X, Xu J, Xu G, Zhang Y, Xia H. Analysis of lymphovascular infiltration and tumor-associated macrophages in cervical cancer immunoescape. *Onco Targets Ther*. 2024;17:1117–1136. doi:10.2147/OTT.S468484
31. Zhang Q, Sioud M. Tumor-associated macrophage subsets: shaping polarization and targeting. *Int J Mol Sci*. 2023;24:7493.
32. Maute R, Xu J, Weissman IL. CD47-SIRPα-targeted therapeutics: status and prospects. *Immunooncol Technol*. 2022;13:100070. doi:10.1016/j.iotech.2022.100070
33. Tigue ML, Loberg MA, Goettel JA, Weiss WA, Lee E, Weiss VL. Wnt signaling in the phenotype and function of tumor-associated macrophages. *Cancer Res*. 2023;83:3–11. doi:10.1158/0008-5472.CAN-22-1403